Long-term meditators self-induce high-amplitude gamma synchrony during mental practice

Antoine Lutz*†, Lawrence L. Greischar*, Nancy B. Rawlings*, Matthieu Ricard‡, and Richard J. Davidson*†

*W. M. Keck Laboratory for Functional Brain Imaging and Behavior, Waisman Center, and Laboratory for Affective Neuroscience, Department of Psychology, University of Wisconsin, 1500 Highland Avenue, Madison, WI 53705; and ‡Shechen Monastery, P.O. Box 136, Kathmandu, Nepal

Communicated by Burton H. Singer, Princeton University, Princeton, NJ, October 6, 2004 (received for review August 26, 2004)

Practitioners understand ''meditation,'' or mental training, to be a process of familiarization with one's own mental life leading to long-lasting changes in cognition and emotion. Little is known about this process and its impact on the brain. Here we find that long-term Buddhist practitioners self-induce sustained electroencephalographic high-amplitude gamma-band oscillations and phase-synchrony during meditation. These electroencephalogram patterns differ from those of controls, in particular over lateral frontoparietal electrodes. In addition, the ratio of gamma-band activity (25–42 Hz) to slow oscillatory activity (4–13 Hz) is initially higher in the resting baseline before meditation for the practitioners than the controls over medial frontoparietal electrodes. This difference increases sharply during meditation over most of the scalp electrodes and remains higher than the initial baseline in the postmeditation baseline. These data suggest that mental training involves temporal integrative mechanisms and may induce short-term and long-term neural changes.

electroencephalogram synchrony | gamma activity | meditation

Little is known about the process of meditation and its impact on the brain (1, 2). Previous studies show the general role of neural synchrony, in particular in the gamma-band frequencies (25–70Hz), in mental processes such as attention, working-memory, learning, or conscious perception (3–7). Such synchronizations of oscillatory neural discharges are thought to play a crucial role in the constitution of transient networks that integrate distributed neural processes into highly ordered cognitive and affective functions (8, 9) and could induce synaptic changes (10, 11). Neural synchrony thus appears as a promising mechanism for the study of brain processes underlining mental training.

Methods

The subjects were eight long-term Buddhist practitioners (mean age, 49 ± 15 years) and 10 healthy student volunteers (mean age, 21 ± 1.5 years). Buddhist practitioners underwent mental training in the same Tibetan Nyingmapa and Kagyupa traditions for 10,000 to 50,000 h over time periods ranging from 15 to 40 years. The length of their training was estimated based on their daily practice and the time they spent in meditative retreats. Eight hours of sitting meditation was counted per day of retreat. Control subjects had no previous meditative experience but had declared an interest in meditation. Controls underwent meditative training for 1 week before the collection of the data.

We first collected an initial electroencephalogram (EEG) baseline consisting of four 60-s blocks of ongoing activity with a balanced random ordering of eyes open or closed for each block. Then, subjects generated three meditative states, only one of which will be described in this report. During each meditative session, a 30-s block of resting activity and a 60-s block of meditation were collected four times sequentially. The subjects were verbally instructed to begin the meditation and meditated at least 20 s before the start of the meditation block. We focus here on the last objectless meditative practice during which both the controls and Buddhist practitioners generated a state of ''unconditional loving-kindness and compassion.''

Meditative Instruction. The state of unconditional loving-kindness and compassion is described as an ''unrestricted readiness and availability to help living beings.'' This practice does not require concentration on particular objects, memories, or images, although in other meditations that are also part of their long-term training, practitioners focus on particular persons or groups of beings. Because ''benevolence and compassion pervades the mind as a way of being,'' this state is called ''pure compassion'' or ''nonreferential compassion'' (*dmigs med snying rje* in Tibetan). A week before the collection of the data, meditative instructions were given to the control subjects, who were asked to practice daily for 1 h. The quality of their training was verbally assessed before EEG collection. During the training session, the control subjects were asked to think of someone they care about, such as their parents or beloved, and to let their mind be invaded by a feeling of love or compassion (by imagining a sad situation and wishing freedom from suffering and well being for those involved) toward these persons. After some training, the subjects were asked to generate such feeling toward all sentient beings without thinking specifically about anyone in particular. During the EEG data collection period, both controls and long-term practitioners tried to generate this nonreferential state of loving-kindness and compassion. During the neutral states, all of the subjects were asked to be in a nonmeditative, relaxed state.

EEG Recordings and Protocol. EEG data were recorded at standard extended 10/20 positions with a 128-channel Geodesic Sensor Net (Electrical Geodesics, Eugene, OR), sampled at 500 Hz, and referenced to the vertex (Cz) with analog band-pass filtering between 0.1 and 200 Hz. EEG signals showing eye movements or muscular artifacts were manually excluded from the study. A digital notch filter was applied to the data at 60 Hz to remove any artifacts caused by alternating current line noise.

Bad channels were replaced by using spherical spline interpolation (12). Two-second epochs without artifact were extracted after the digital rereferencing to the average reference.

Spectral Analysis. For each electrode and for each 2-s epoch, the power spectral distribution was computed by using Welch's method (13), which averages power values across sliding and overlapping 512-ms time windows. To compute the relative gamma activity, the power spectral distribution was computed on the z-transformed EEG by using the mean and SD of the signal in each 2-s window. This distribution was averaged through all electrodes, and the ratio between gamma and slow rhythms was computed. Intraindividual analyses were run on this measure and a group analysis was run on the average ratio across 2-s windows. The group analysis of the topography was performed by averaging the power spectral distribution for each electrode

Freely available online through the PNAS open access option.

Abbreviations: ROI, region of interest; EEG, electroencephalogram.

†To whom correspondence may be addressed. E-mail: alutz@wisc.edu or rjdavids@wisc.edu.

in each block and then computing the ratio of gamma to slow rhythms before averaging across blocks.

Despite careful visual examination, the electroencephalographic spectral analysis was hampered by the possible contamination of brain signals by muscle activity. Here we assume that the spectral emission between 80 and 120 Hz provided an adequate measure of the muscle activity (14, 15). The muscle EEG signature is characterized by a broad-band spectrum profile (8–150 Hz) peaking at 70–80 Hz (16). Thus, the variation through time of the average spectral power in the 80–120 Hz frequency band provided a way to quantify the variations of the muscle contribution to the EEG gamma activity through time. To estimate the gamma activity, adjusted for the very high frequencies, we performed a covariance analysis for each region of interest (ROI) for each subject. The dependent variable was the average gamma activity (25–42 Hz) in each ROI. The continuous predictor was the electromyogram activity (80–120 Hz power). The categorical predictors were the blocks (initial baseline with eyes open and neutral blocks from 2 to 4) and the mental states (ongoing neutral versus meditation).

For the group analysis, separate repeated ANOVAs were then performed on the relative gamma and adjusted gamma variation between states, with the blocks as the within factor and the group (practitioners versus controls) as the categorical predictor. For the intrasubject analysis, we compared separately the relative gamma and the raw gamma activity averaged within the ROIs in the initial baseline state versus the meditative state.

Phase-Synchrony Detection. Electrodes of interest were referenced to a local average potential defined as the average potential of its six surrounding neighbors. This referencing montage restricted the electrical measurement to local sources only and prevented spurious long-range synchrony from being detected if the muscle activity over one electrode propagated to another distant electrode. The methods used to measure long-range synchronization are described in detail in *Supporting Methods*, which is published as supporting information on the PNAS web site. In summary, for each epoch and electrode, the instantaneous phase of the signal was extracted at each frequency band between 25 and 42 Hz in 2-Hz steps by using a convolution with Morlet wavelets. The stability through time of their phase difference was quantified in comparison with white-noise signals as independent surrogates. A measure of synchronous activity was defined as the number of electrode pairs among the 294 studied combinations that had higher synchrony density on average across frequencies than would be expected to occur between independent signals. The electrode pairs were taken between the ROIs when we measured the scalp distribution of gamma activity (see Fig. 3*a*). A repeated-measures ANOVA was performed on the average size of the synchrony pattern across all frequency bands and epochs in each block with the original resting state and the meditative state as the within factors and the group (practitioners versus controls) as the between-groups factor.

Results

We first computed the power spectrum density over each electrode in the EEG signals visually free from artifacts. This procedure was adapted to detect change in local synchronization (6, 9). Local synchronization occurs when neurons recorded by a single electrode transiently oscillate at the same frequency with a common phase: Their local electric field adds up to produce a burst of oscillatory power in the signal reaching the electrode. Thus, the power spectral density provides an estimation of the average of these peaks of energy in a time window. During meditation, we found high-amplitude gamma oscillations in the EEGs of long-time practitioners (subjects S1–S8) that were not present in the initial baseline.

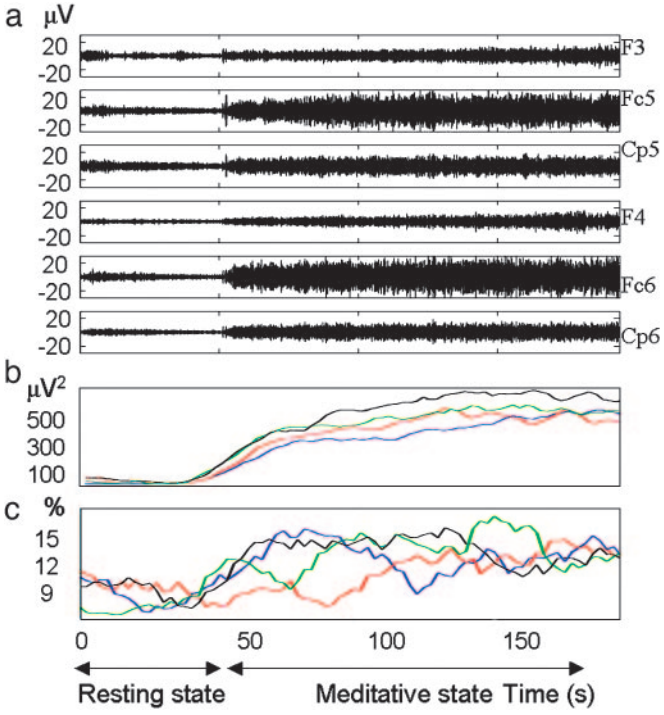

Fig. 1. High-amplitude gamma activity during mental training. (*a*) Raw electroencephalographic signals. At $t = 45$ s, practitioner S4 started generating a state of nonreferential compassion, block 1. (*b*) Time course of gamma activity power over the electrodes displayed in *a* during four blocks computed in a 20-s sliding window every 2 s and then averaged over electrodes. (*c*) Time course of subjects' cross-hemisphere synchrony between 25 and 42 Hz. The density of long-distance synchrony above a surrogate threshold was calculated in a 20-s sliding window every 2 s for each cross-hemisphere electrode pair and was then averaged across electrode pairs (see *Methods*). Colors denote different trial blocks: blue, block 1; red, block 2; green, block 3; black, block 4.

Fig. 1*a* provides a representative example of the raw EEG signal (25–42 Hz) for subject S4. An essential aspect of these gamma oscillations is that their amplitude monotonically increased over the time of the practice (Fig. 1*b*).

Relative Gamma Power. We characterized these changes in gamma oscillations in relation to the slow rhythms (4–13 Hz) that are thought to play a complementary function to fast rhythms (3). Fig. 2*a* shows the intraindividual analysis of this ratio averaged through all electrodes. This ratio, which was averaged across all electrodes, presented an increase compared with the initial baseline, which was greater than twice the baseline SD for two controls and all of the practitioners. The ratio of gamma-band activity (25–42 Hz) compared to slow rhythms was initially higher in the baseline before meditation for the practitioners compared with the controls ($t = 4.0$, df = 16, $P < 0.001$; t test) (Fig. 2*b*). This effect remained when we compared the three youngest practitioners with the controls (25, 34, and 36 years old, respectively) ($t = 2.2$, df = 11, $P < 0.05$; t test). This result suggests that the mean age difference between groups does not fully account for this baseline difference (17).

This baseline difference increased sharply during meditation, as revealed by an interaction between the state and group factors [$F(2, 48) = 3.7, P < 0.05$; ANOVA] (Fig. 2*b*). This difference was still found in comparisons between gamma activity and both theta (4–8 Hz) and alpha activity. To localize these differences on the scalp, similar analyses were performed on each individual electrode. Fig. 2*c* shows a higher ratio of fast versus slow

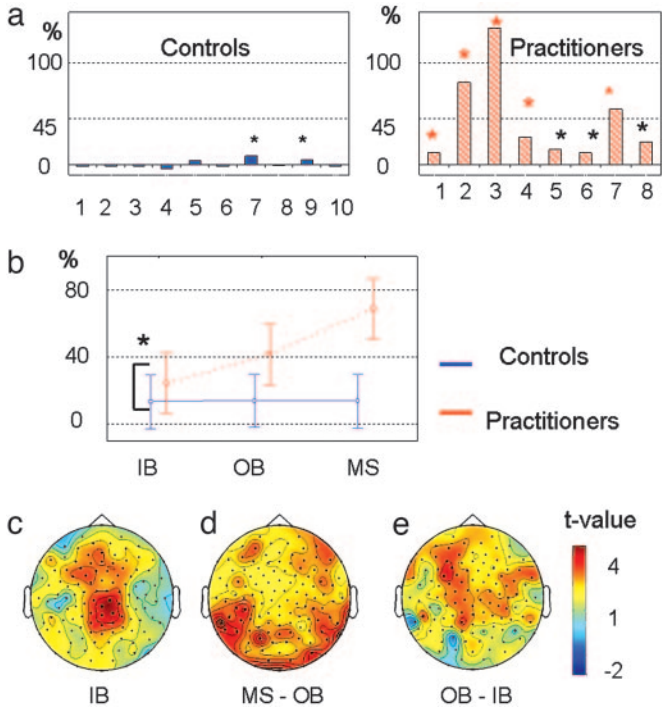

Fig. 2. Relative gamma power during mental training. (*a* and *b*) Intraindividual analysis on the ratio of gamma (25–42 Hz) to slow (4–13 Hz) oscillations averaged through all electrodes. (*a*) The abscissa represents the subject numbers, the ordinate represents the difference in the mean ratio between the initial state and meditative state, and the black and red stars indicate that this increase is >2- and 3-fold, respectively, the baseline SD. (*b*) Interaction between the subject and the state factors for this ratio [$F(2, 48) = 3.5$, $P < 0.05$; ANOVA]. IB, initial baseline; OB, ongoing baseline; MS, meditative state. (*c*–*e*) Comparisons of this ratio between controls and practitioners over each electrode [$t > 2.6$, $P < 0.01$, scaling ($-2.5, 4$); *t* test] during the premeditative initial baseline (*c*), between the ongoing baseline and the meditative state (*d*), and between the ongoing baseline and the initial baseline (*e*).

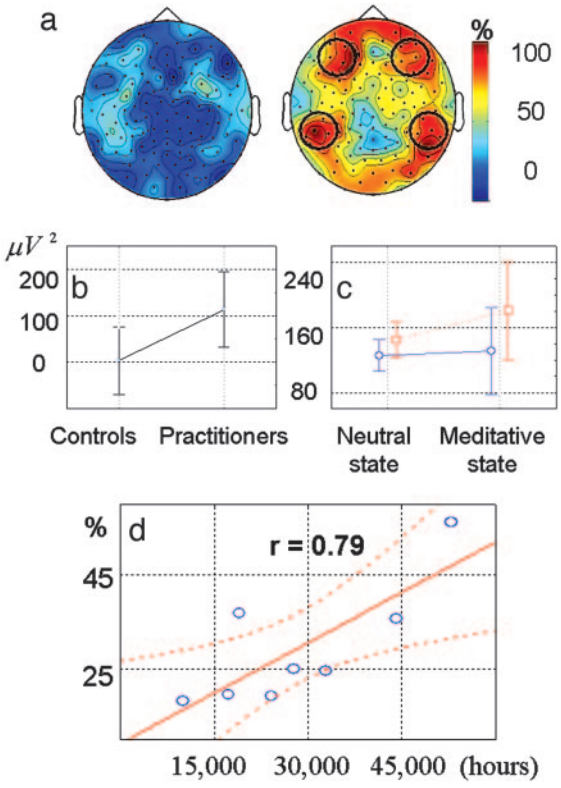

Fig. 3. Absolute gamma power and long-distance synchrony during mental training. (*a*) Scalp distribution of gamma activity during meditation. The color scale indicates the percentage of subjects in each group that had an increase of gamma activity during the mental training. (*Left*) Controls. (*Right*) Practitioners. An increase was defined as a change in average gamma activity of >1 SD during the meditative state compared with the neutral state. Black circles indicate the electrodes of interest for the group analysis. (*b*) Adjusted gamma variation between neutral and meditative states over electrodes F3-8, Fc3-6, T7-8, Tp7-10, and P7-10 for controls and long-time practitioners [$F(1, 16) = 4.6$, $P < 0.05$; ANOVA]. (*c*) Interaction between the group and state variables for the number of electrode pairs between ROIs that exhibited synchrony higher than noise surrogates [$F(1, 16) = 6.5$, $P < 0.05$; ANOVA]. The blue line represents the controls; the red line represents the practitioners. (*d*) Correlation between the length of the long-term practitioners' meditation training and the ratio of relative gamma activity averaged across electrodes in the initial baseline ($P < 0.02$). Dotted lines represent 95% confidence intervals.

oscillations for the long-term practitioners versus the controls in the initial baseline over medial frontoparietal electrodes ($t > 2.59$, $P = 0.01$; *t* test). Similarly, Fig. 2*d* shows a group difference between the ongoing baseline states and the meditative state, in particular over the frontolateral and posterior electrodes. Interestingly, the postmeditative baseline (neutral states in blocks 2, 3, and 4) also revealed a significant increase in this ratio compared with the premeditation baseline over mainly anterior electrodes (Fig. 2*e*).

These data suggest that the two groups had different electrophysiological spectral profiles in the baseline, which are characterized by a higher ratio of gamma-band oscillatory rhythm to slow oscillatory rhythms for the long-term practitioners than for the controls. This group difference is enhanced during the meditative practice and continues into the postmeditative resting blocks.

Absolute Gamma Power. We then studied the variation through time of the ongoing gamma-band activity itself. The gamma-band activity (25–42 Hz) was first *z*-transformed in each block and compared over each electrode with the mean and SD of their respective neutral block (ongoing baseline). The normalized gamma activity was then averaged across the blocks. Fig. 3*a* shows the percentage of subjects presenting an increase of at least 1 SD during meditation compared with neutral state. A common topographical pattern of gamma activity emerged across the long-term practitioners but not across the control subjects. This pattern was located bilaterally over the parieto-temporal and midfrontal electrodes. Fig. 3*a* shows four ROIs containing seven electrodes each and located around F3-8, Fc3-6, T7-8, Tp7-10, and P7-10. Hereafter, we focus on the electrodes activated in these ROIs.

Intraindividual analyses similar to those for relative gamma activity were run on the average gamma power across these ROIs and exhibited the same pattern as that found for relative gamma. It is possible that these high-amplitude oscillations are partially contaminated by muscle activity (18). Because we found increases in gamma activity during the postmeditative resting baseline compared with the initial resting baseline, it is unlikely that the changes we reported could be solely caused by muscle activity, because there was little evidence of any muscle activity during these baseline periods. (Fig. 2*e*). Secondly, we showed that the meditative state and nonmeditative state that mimicked and exaggerated the possible muscle activity during meditation exhibit significantly different spectral profiles (Fig. 4, which is published as supporting information on the PNAS web site). Furthermore, for the two subjects showing the highest gamma activity, we showed that amplitude of the gamma-band activity before external stimulation predicts the amplitude of high fast-

frequency oscillations (20–45 Hz) evoked by auditory stimuli (Fig. 5, which is published as supporting information on the PNAS web site). Because the evoked activity is relatively independent of muscle activity, the relationship between the prestimulation fast-frequency oscillation and the evoked activity suggests that these high-amplitude gamma rhythms are not muscle artifacts (Fig. 5 and Fig. 6, which is published as supporting information on the PNAS web site). This claim is further supported by the localization within the brain of the dipole sources of these fast-frequency-evoked oscillations (Figs. 7–9, which are published as supporting information on the PNAS web site).

Yet we still chose to cautiously interpret the raw values of these gamma oscillations because of the concomitant increase of spectral power >80 Hz during meditation. This increase could also reflect a change in muscle activity rather than high-frequency, gamma-band oscillations [70–105 Hz (19)], which are mostly low-pass filtered by the skull at >80 Hz. Thus, we chose to conservatively interpret the activity at >80 Hz as indicating muscle activity.

To remove the contribution of putative muscle activity, we quantified the increase in the average amplitude of gamma oscillation (25–42 Hz) adjusted for the effect of the very high-frequency variation (80–120 Hz) (see *Methods* and ref. 20). The adjusted average variation in gamma activity was >30-fold greater among practitioners compared with controls (Fig. 3*b*). Group analysis was run on the average adjusted gamma activity over these ROIs. Gamma activity increased for both the long-term practitioners and controls from neutral to meditation states [$F(1, 16) = 5.2, P < 0.05$; ANOVA], yet this increase was higher for the long-time practitioners than for the controls [$F(1, 16) = 4.6, P < 0.05$; interaction between the state and group factors ANOVA] (Fig. 3*b*). In summary, the generation of this meditative state was associated with gamma oscillations that were significantly higher in amplitude for the group of practitioners than for the group of control subjects.

Long-Distance Gamma Synchrony. Finally, a long-distance synchrony analysis was conducted between electrodes from the ROIs found in Fig. 3*a*. Long-distance synchrony is thought to reflect large-scale neural coordination (9) and can occur when two neural populations recorded by two distant electrodes oscillate with a precise phase relationship that remains constant during a certain number of oscillation cycles. This approach is illustrated in Fig. 1*c* for selected electrodes (F3/4, Fc5/6, and Cp5/6). For subject S4, the density of cross-hemisphere, long-distance synchrony increases by ≈30% on average during meditation and follows a pattern similar to the oscillatory gamma activity.

For all subjects, locally referenced, long-distance synchronies were computed for each 2-s epoch during the neutral and meditative states between all electrode pairs and across eight frequencies ranging from 25 to 42 Hz. In each meditative or neutral block, we counted the number of electrode pairs (294 electrode pairs maximum) that had an average density of synchrony higher than those derived from noise surrogates (see *Methods*). We ran a group analysis on the size of the synchronous pattern and found that its size was greater for long-time practitioners than for controls [$F(1, 16) = 10.3, P < 0.01$; ANOVA] and increased from neutral to meditation states [$F(1, 16) = 8.2, P < 0.02$; ANOVA]. Fig. 3*c* shows that the group and state factors interacted on long-distance synchrony [$F(1, 16) = 6.5, P < 0.05$; ANOVA]: The size of synchrony patterns increased more for the long-time practitioners than for the controls from neutral to meditation states. These data suggest that large-scale brain coordination increases during mental practice.

Finally, we investigated whether there was a correlation between the hours of formal sitting meditation (for subjects S1–S8, 9,855–52,925 h) and these electrophysiological measures for the long-term practitioners, in either the initial or meditative states (same values as in Figs. 2 and 3). The correlation coefficients for the relative, absolute, and phase-synchrony gamma measures were positive: $r = 0.79$, 0.63, and 0.64, respectively, in the initial state, and $r = 0.66$, 0.62, and 0.43, respectively, in the meditative state. A significant positive correlation was found only in the initial baseline for the relative gamma ($r = 0.79, P < 0.02$) (Fig. 3*d*). These data suggest that the degree of training can influence the spectral distribution of the ongoing baseline EEG. The age of the subject was not a confounding factor in this effect as suggested by the low correlation between the practitioner age and the relative gamma ($r = 0.23$).

Discussion

We found robust gamma-band oscillation and long-distance phase-synchrony during the generation of the nonreferential compassion meditative state. It is likely based on descriptions of various meditation practices and mental strategies that are reported by practitioners that there will be differences in brain function associated with different types of meditation. In light of our initial observations concerning robust gamma oscillations during this compassion meditation state, we focused our initial attention on this state. Future research is required to characterize the nature of the differences among types of meditation. Our resulting data differ from several studies that found an increase in slow alpha or theta rhythms during meditation (21). The comparison is limited by the fact that these studies typically did not analyze fast rhythms. More importantly, these studies mainly investigated different forms of voluntary concentrative meditation on an object (such as a meditation on a mantra or the breath). These concentration techniques can be seen as a particular form of top-down control that may exhibit an important slow oscillatory component (22). First-person descriptions of objectless meditations, however, differ radically from those of concentration meditation. Objectless meditation does not directly attend to a specific object but rather cultivates a state of being. Objectless meditation does so in such a way that, according to reports given after meditation, the intentional or object-oriented aspect of experience appears to dissipate in meditation. This dissipation of focus on a particular object is achieved by letting the very essence of the meditation that is practiced (on compassion in this case) become the sole content of the experience, without focusing on particular objects. By using similar techniques during the practice, the practitioner lets his feeling of loving-kindness and compassion permeate his mind without directing his attention toward a particular object. These phenomenological differences suggest that these various meditative states (those that involve focus on an object and those that are objectless) may be associated with different EEG oscillatory signatures.

The high-amplitude gamma activity found in some of these practitioners are, to our knowledge, the highest reported in the literature in a nonpathological context (23). Assuming that the amplitude of the gamma oscillation is related to the size of the oscillating neural population and the degree of precision with which cells oscillate, these data suggest that massive distributed neural assemblies are synchronized with a high temporal precision in the fast frequencies during this state. The gradual increase of gamma activity during meditation is in agreement with the view that neural synchronization, as a network phenomenon, requires time to develop (24), proportional to the size of the synchronized neural assembly (25). But this increase could also reflect an increase in the temporal precision of the thalamocortical and corticocortical interactions rather than a change in the size of the assemblies (8). This gradual increase also corroborates the Buddhist subjects' verbal report of the chronometry of their practice. Typically, the transition from the neutral

state to this meditative state is not immediate and requires 5–15 s, depending on the subject. The endogenous gamma-band synchrony found here could reflect a change in the quality of moment-to-moment awareness, as claimed by the Buddhist practitioners and as postulated by many models of consciousness (26, 27).

In addition to the meditation-induced effects, we found a difference in the normative EEG spectral profile between the two populations during the resting state before meditation. It is not unexpected that such differences would be detected during a resting baseline, because the goal of meditation practice is to transform the baseline state and to diminish the distinction between formal meditation practice and everyday life. Moreover, Gusnard and Raichle (28) have highlighted the importance of characteristic patterns of brain activity during the resting state and argue that such patterns affect the nature of task-induced changes. The differences in baseline activity reported here suggest that the resting state of the brain may be altered by long-term meditative practice and imply that such alterations may affect task-related changes. Our practitioners and control subjects differed in many respects, including age, culture of origin, and first language, and they likely differed in many more respects, including diet and sleep. We examined whether age was an important factor in producing the baseline differences we observed by comparing the three youngest practitioners with the controls and found that the mean age difference between groups is unlikely the sole factor responsible for this baseline difference. Moreover, hours of practice but not age significantly predicted relative gamma activity during the initial baseline period. Whether other demographic factors are important in producing these effects will necessarily require further research, particularly longitudinal research that follows individuals over time in response to mental training.

Our study is consistent with the idea that attention and affective processes, which gamma-band EEG synchronization may reflect, are flexible skills that can be trained (29). It remains for future studies to show that these EEG signatures are caused by long-term training itself and not by individual differences before the training, although the positive correlation that we found with hours of training and other randomized controlled trials suggest that these are training-related effects (2). The functional consequences of sustained gamma-activity during mental practice are not currently known but need to be studied in the future. The study of experts in mental training may offer a promising research strategy to investigate high-order cognitive and affective processes (30).

We thank J. Dunne for Tibetan translation; A. Shah, A. Francis, and J. Hanson for assistance in data collection and preanalysis; the long-time Buddhist practitioners who participated in the study; J.-Ph. Lachaux, J. Martinerie, W. Singer, and G. Tononi and his team for suggestions on the manuscript; F. Varela for early inspirations; and His Holiness the Dalai Lama for his encouragement and advice in the conducting of this research. We also thank the Mind and Life Institute for providing the initial contacts and support to make this research possible. This research was supported by National Institute of Mental Health Mind-Body Center Grant P50-MH61083, the Fyssen Foundation, and a gift from Edwin Cook and Adrianne Ryder-Cook.

1. Austin, J. H. (1998) *Zen and the Brain: Toward an Understanding of Meditation and Consciousness* (MIT Press, Cambridge, MA).
2. Davidson, R. J., Kabat-Zinn, J., Schumacher, J., Rosenkranz, M., Muller, D., Santorelli, S. F., Urbanowski, F., Harrington, A., Bonus, K. & Sheridan, J. F. (2003) *Psychosom. Med.* **65,** 564–570.
3. Fries, P., Reynolds, J. H., Rorie, A. E. & Desimone, R. (2001) *Science* **291,** 1560–1563.
4. Miltner, W. H., Braun, C., Arnold, M., Witte, H. & Taub, E. (1999) *Nature* **397,** 434–436.
5. Srinivasan, R., Russell, D. P., Edelman, G. M. & Tononi, G. (1999) *J. Neurosci.* **19,** 5435–5448.
6. Tallon-Baudry, C., Bertrand, O., Peronnet, F. & Pernier, J. (1998) *J. Neurosci.* **18,** 4244–4254.
7. Rodriguez, E., George, N., Lachaux, J. P., Martinerie, J., Renault, B. & Varela, F. J. (1999) *Nature* **397,** 430–433.
8. Singer, W. (1999) *Neuron* **24,** 49–65.
9. Varela, F., Lachaux, J. P., Rodriguez, E. & Martinerie, J. (2001) *Nat. Rev. Neurosci.* **2,** 229–239.
10. Hebb, D. O. (1949) *The Organization of Behavior: A Neuropsychological Theory* (Wiley, New York).
11. Paulsen, O., Sejnowski, T. J. (2000) *Curr. Opin. Neurobiol.* **10,** 172–179.
12. Perrin, F., Pernier, J., Bertrand, O. & Echallier, J. F. (1989) *Electroencephalogr. Clin. Neurophysiol.* **72,** 184–187.
13. Welch, P. D. (1967) *IEEE Trans. Audio Electroacoust.* **15,** 70–73.
14. Davidson, R. J., Marshall, J. R., Tomarken, A. J. & Henriques, J. B. (2000) *Biol. Psychiatry* **47,** 85–95.
15. Pivik, R. T., Broughton, R. J., Coppola, R., Davidson, R. J., Fox, N. & Nuwer, M. R. (1993) *Psychophysiology* **30,** 547–558.
16. Cacioppo, J. T., Tassinary, L. G. & Fridlund, A. J. (1990) in *Principles of Psychophysiology*, ed. Tassinary, L. G. (Cambridge Univ. Press, New York), pp. 325–384.
17. Duffy, F. H., Albert, M. S., McAnulty, G. & Garvey, A. J. (1984) *Ann. Neurol.* **16,** 430–438.
18. Goncharova, I. I., McFarland, D. J., Vaughan, T. M. & Wolpaw, J. R. (2003) *Clin. Neurophysiol.* **114,** 1580–1593.
19. Herculano-Houzel, S., Munk, M. H., Neuenschwander, S. & Singer, W. (1999) *J. Neurosci.* **19,** 3992–4010.
20. Davidson, R. J., Jackson, D. C. & Larson, L. C. (2000) in *Handbook of Psychophysiology* (Cambridge Univ. Press, New York), pp. 27–52.
21. Shapiro, D. H. (1980) *Meditation: Self-Regulation Strategy and Altered State of Consciousness* (Aldine, New York).
22. von Stein, A., Chiang, C. & Konig, P. (2000) *Proc. Natl. Acad. Sci. USA* **97,** 14748–14753.
23. Baldeweg, T., Spence, S., Hirsch, S. R. & Gruzelier, J. (1998) *Lancet* **352,** 620–621.
24. Kuramato, Y. (1975) in *International Symposium on Mathematical Problems in Theoretical Physics*, ed. Araki, H. (Springer, New York), Vol. 39, pp. 420.
25. Campbell, S. R., Wang, D. L. & Jayaprakash, C. (1999) *Neural Comput.* **11,** 1595–1619.
26. Tononi, G. & Edelman, G. M. (1998) *Science* **282,** 1846–1851.
27. Engel, A. K., Fries, P., Konig, P., Brecht, M. & Singer, W. (1999) *Conscious. Cognit.* **8,** 128–151.
28. Gusnard, D. A. & Raichle, M. E. (2001) *Nat. Rev. Neurosci.* **2,** 685–694.
29. Posner, M. I., DiGirolamo, G. J. & Fernandez-Duque, D. (1997) *Conscious. Cognit.* **6,** 267–290.
30. Lutz, A. & Thompson, E. (2003) *J. Conscious. Stud.* **10,** 31–52.

Supporting Methods

Neural synchrony is an important candidate for large-scale integration. The current assumption is that distant functional areas mediated by neuronal groups that oscillate in specific frequency bands enter into precise phase-locking over a limited period of time during cognitive and emotional activity. In this study, we applied a method that directly estimates long-distance phase synchrony as a function of time in frequency bands of interest (here, the gamma band). In this context, it is important to distinguish between synchrony as a proper estimate of phase relation and the classical measures of spectral covariance or coherence (1). As practiced, coherence has two important limitations for our purposes. *(i)* The classical tools for measuring coherence based on Fourier analysis are highly dependent on the stationarity of the measured signal, which is far from being the case in the brain. *(ii)* Coherence is a measure of spectral covariance and thus does not separate the effects of amplitude and phase in the interrelations between two signals. Because we are interested in exploring the explicit hypothesis that phase-locking synchrony is the relevant biological mechanism of brain integration, coherence provides only an indirect measure. Furthermore, in some experiments, external factors, such as respiration or heartbeat, may create amplitude modulations, and one would like to exclude these sources of coherence to focus solely on phase difference.

In this article, we estimated the effect of meditation on long-distance synchrony in four steps. In the first step we measured the instantaneous phase of the signals around the frequency of interest (frequencies between 25 and 42 Hz in 2-Hz steps). The phase of the signals was extracted from the coefficients of their wavelet transform. More precisely, let an electrode record a neural signal $x(u)$, then these wavelet coefficients as

a function of time (τ) and frequency (*f*) were defined as: $\Psi_{\tau,f}(u) = \sqrt{f}.\exp(i2\pi f(u-\tau)).\exp(-\frac{(u-\tau)^2}{\sigma^2})$.

$\Psi_{\tau,f}(u)$ was simply the product of a sinusoidal wave at frequency *f*, with a Gaussian function centered at time (τ) with a standard deviation, σ, proportional to the inverse of *f*. The temporal resolution of this wavelet was defined by the number of oscillations of the sinusoidal wave (here, six cycles). The wavelet transform of a signal $x(u)$ was a function of time (τ) and frequency (*f*) given by the convolution of *x* with this wavelet family: $W_x(\tau,f) = \int_{-\infty}^{+\infty} x(u).\Psi_{\tau,f}{}^*(u)du$.

Now, as a second step, the phase difference between the signals *x* and *y* at frequency (*f*) and time (τ) was derived from the angles of their wavelet coefficients: $\exp(j(\phi_y(f,\tau) - \phi_x(f,\tau))) = \frac{W_{y'f}(\tau)}{|W_{y'f}(\tau)|}.\frac{W^*_{x'f}(\tau)}{|W_{x'f}(\tau)|}$. The stability of the coupling was estimated by quantifying the phase-locking value (PLV) across eight cycles of oscillation at the frequency (*f*) at any given time *t*. $PLV(f,t) = \left|\frac{1}{\delta}\int_{t-\delta/2}^{t+\delta/2}\exp(j(\phi_y(f,\tau) - \phi_x(f,\tau)))d\tau\right|$.

As a third step, the PLV measure was compared with the distribution of PLV values obtained for 1,000 pairs of independent surrogate white-noise signals. This comparison was used to determine the episodes of significantly higher synchrony than what would be expected to occur between independent signals (P<0.05).

As a fourth and final step, the density of PLV above threshold was computed in any given 2-s window for each electrode pair and for each frequency band between 25 and 42 Hz (in 2-Hz steps). Then we counted the number of electrode pairs with a

density that exceeded a significance level of $P<0.05$. Because there were six possible combinations between the four regions of interest (ROI) from Fig. 3a and because each ROI contains seven electrodes that can be paired with one of the seven electrodes from another ROI, the total number of combinations of electrode pairs was 294 (6*7*7). Intraindividual and group analyses were then performed on this measure as described in the method section.

1. Carter, C. (1987) *Proc. IEEE* **75,** 236-255.

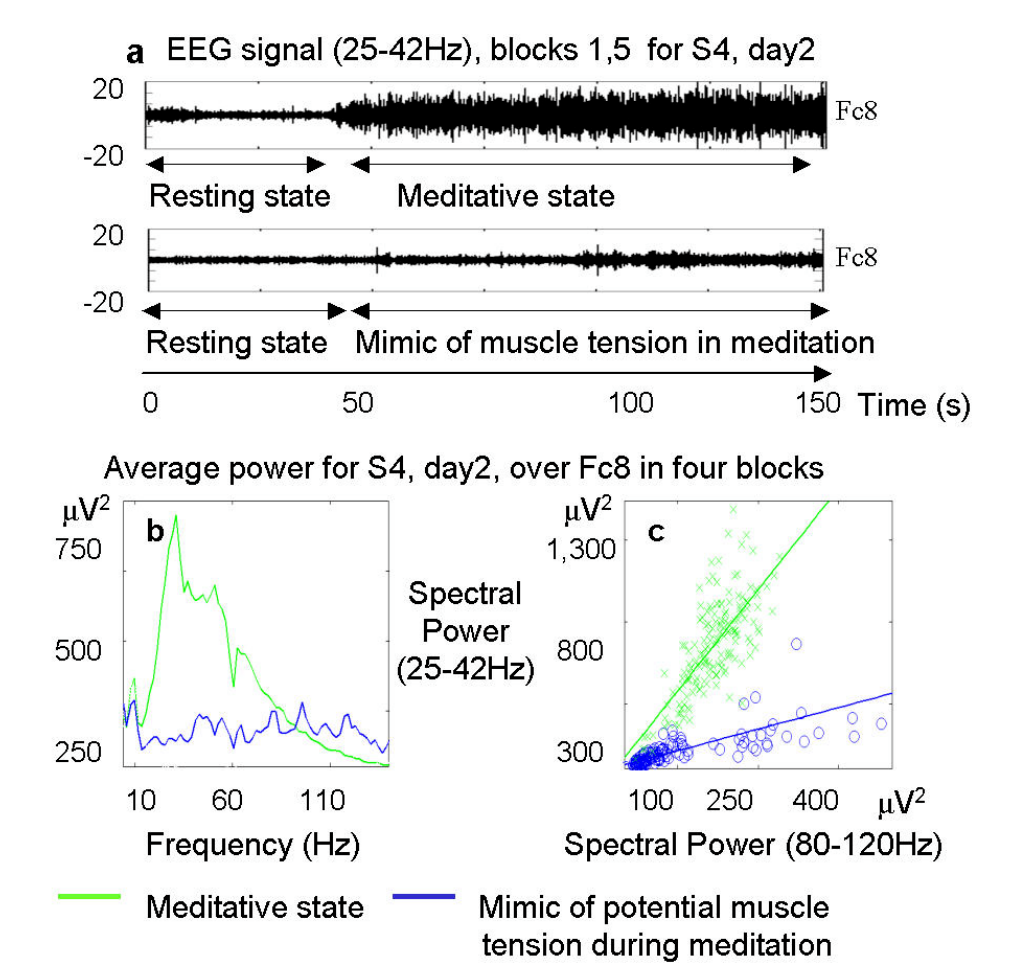
a EEG signal (25-42Hz), blocks 1,5 for S4, day2
20
-20
Fc8
Resting state
Meditative state
20
-20
Fc8
Resting state
Mimic of muscle tension in meditation
0
50
100
150
Time (s)
Average power for S4, day2, over Fc8 in four blocks
μV²
750
500
250
b
10
60
110
Frequency (Hz)
Spectral Power (25-42Hz)
μV²
1,300
800
300
c
100
250
400
μV²
Spectral Power (80-120Hz)
Meditative state
Mimic of potential muscle tension during meditation

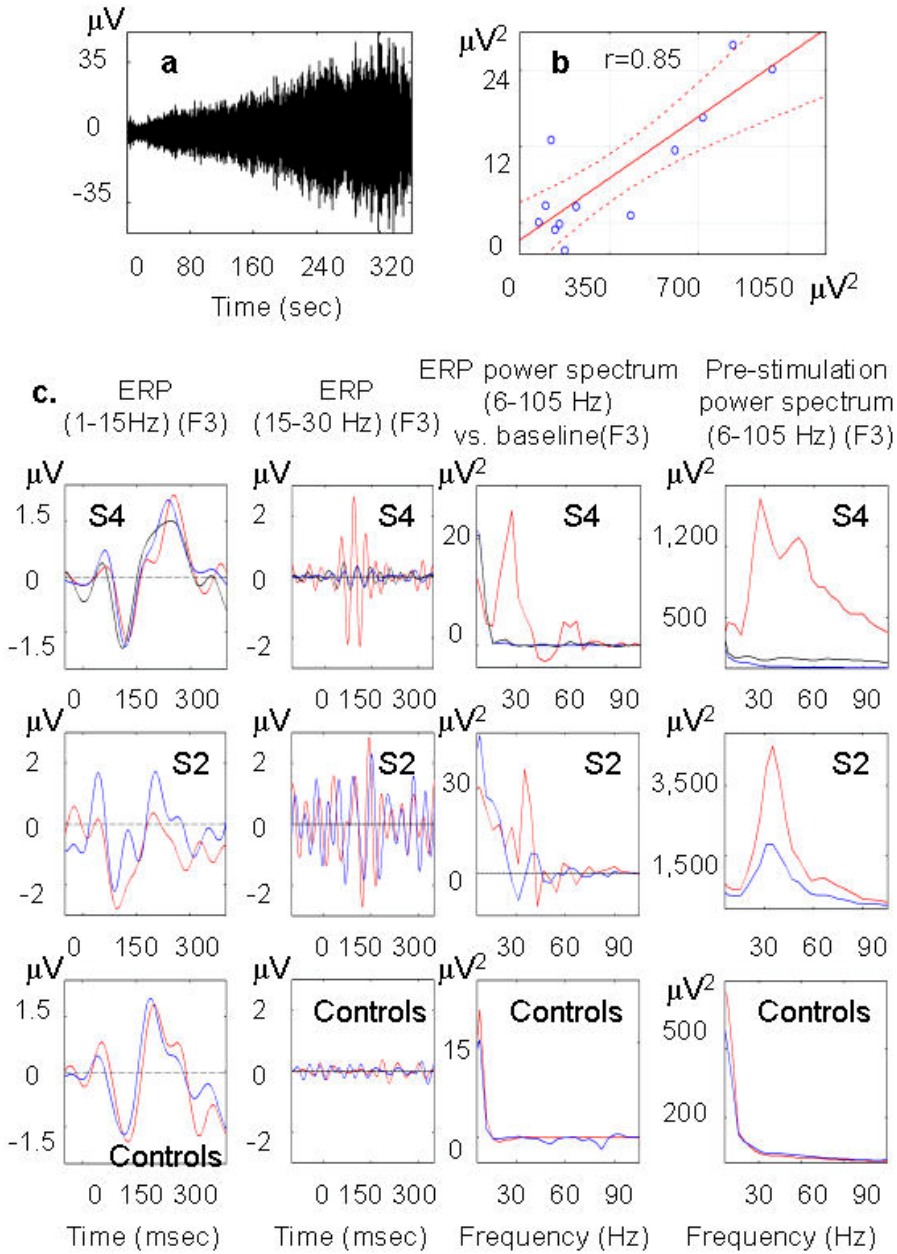
μV
35
a
0
-35
0 80 160 240 320
Time (sec)
μV²
24
b
r=0.85
12
0
0 350 700 1050 μV²
c.
ERP (1-15Hz) (F3)
ERP (15-30 Hz) (F3)
ERP power spectrum (6-105 Hz) vs. baseline(F3)
Pre-stimulation power spectrum (6-105 Hz) (F3)
S4
S2
Controls
Time (msec)
Time (msec)
Frequency (Hz)
Frequency (Hz)
Open presence
Concentration on a visual object
Reading

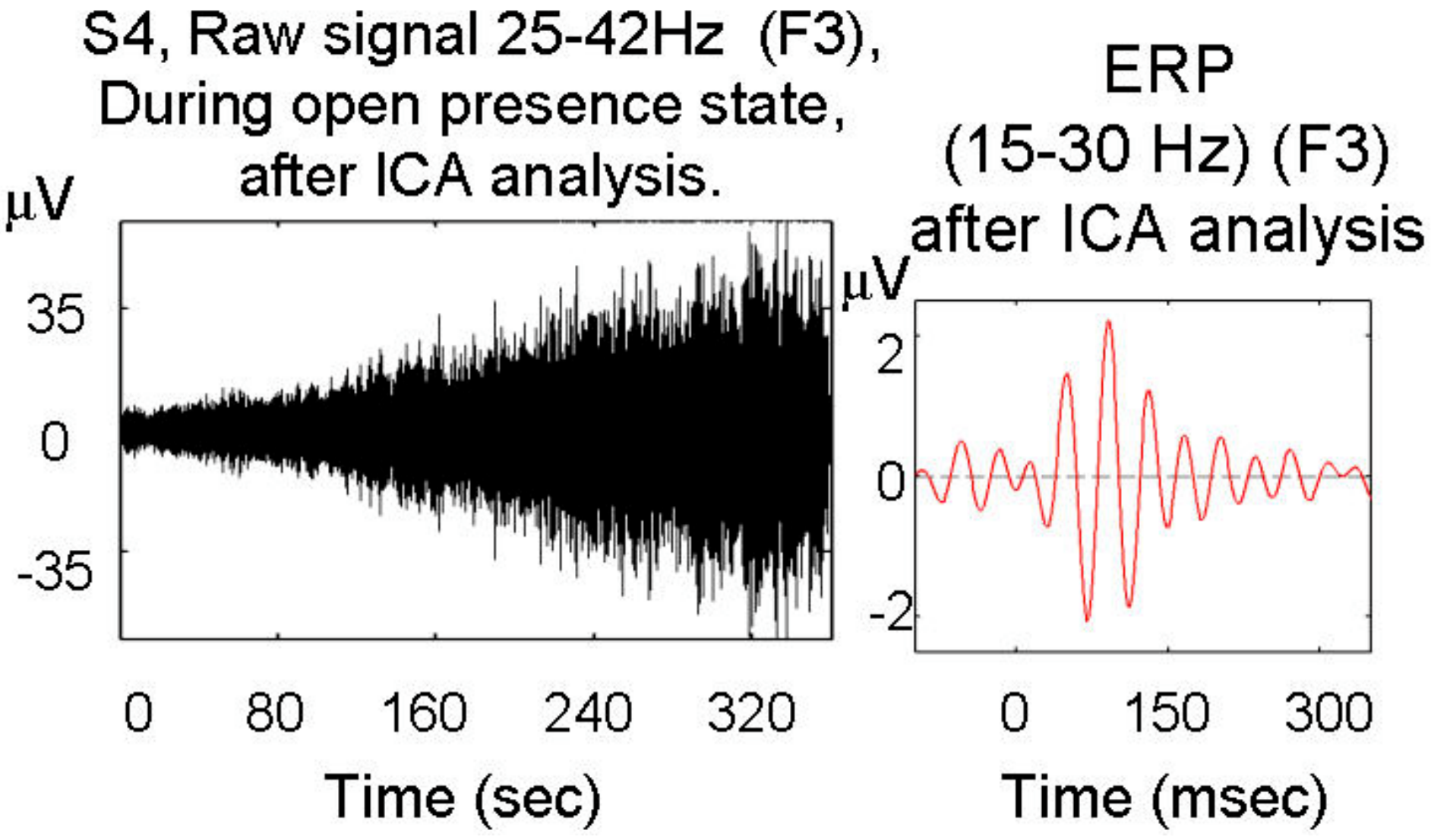
S4, Raw signal 25-42Hz (F3),
During open presence state,
after ICA analysis.
μV
35
0
-35
0
80
160
240
320
Time (sec)
ERP
(15-30 Hz) (F3)
after ICA analysis
μV
2
0
-2
0
150
300
Time (msec)

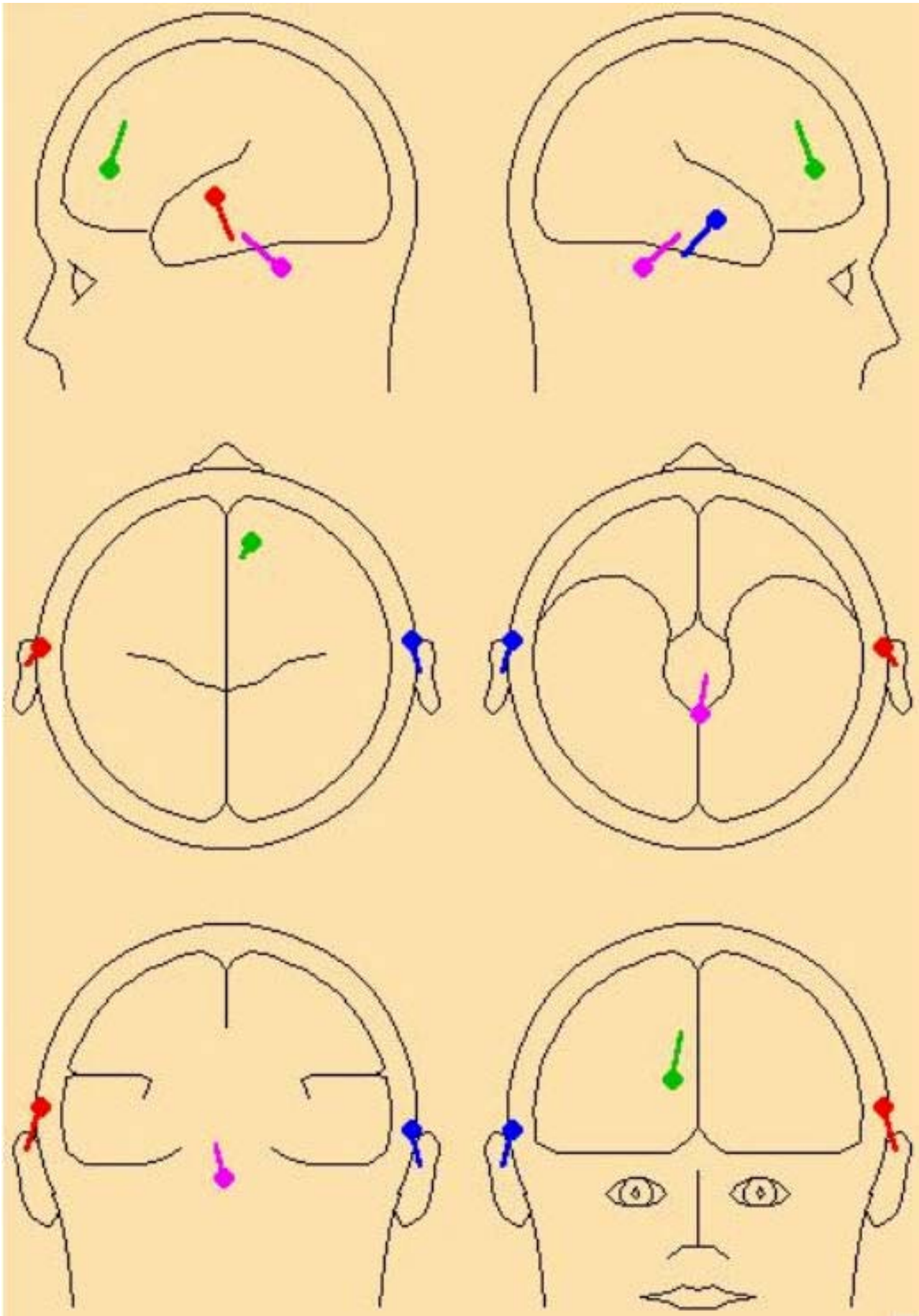

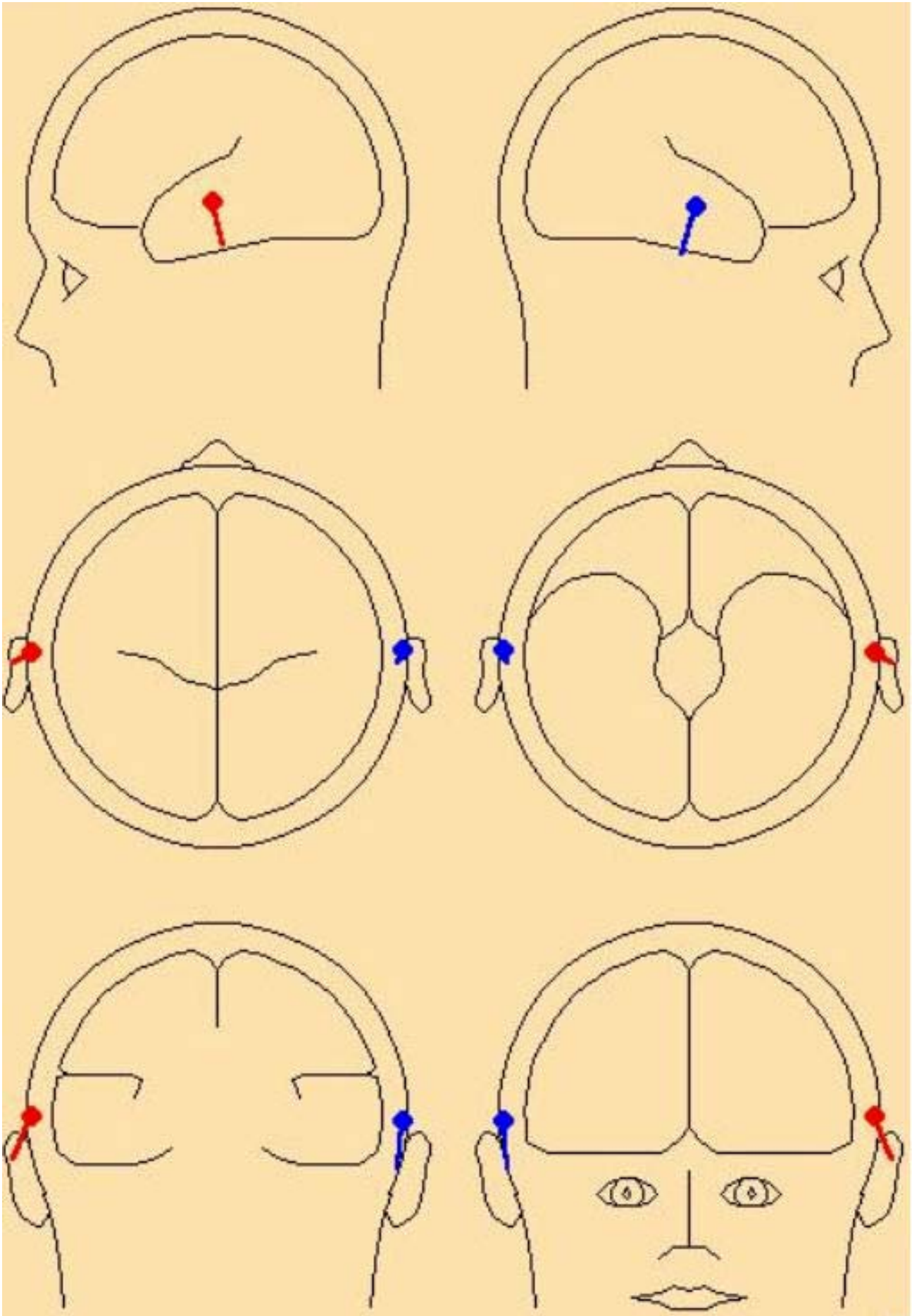

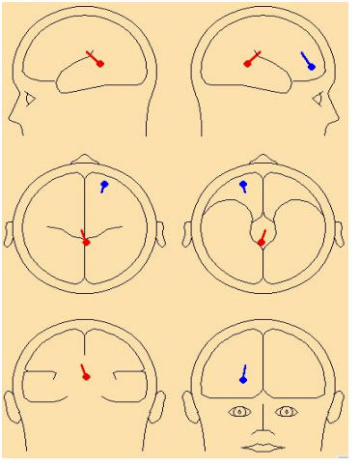
a
b
SAG
COR
TRA
A
P
R
L
a